

THE ROLE OF SOLAR WIND HYDROGEN IN SPACE WEATHERING: INSIGHTS FROM LABORATORY-IRRADIATED NORTHWEST AFRICA 12008. M. L. Shusterman¹, T. G. Sharp¹, M. S. Robinson¹, Z. Rahman², L. P. Keller², C. A. Dukes³, C. Bu³ and M. A. Roldan⁴, ¹School of Earth and Space Exploration, Arizona State University (E-mail: Morgan.Shusterman@asu.edu). ²ARES, XI3, NASA/JSC. ³Laboratory for Astrophysics and Surface Physics, University of Virginia, ⁴Eyring Materials Center, Arizona State University.

Introduction: Micrometeoroid impacts, solar wind plasma interactions, and regolith gardening drive the complicated and nuanced mechanism of space weathering (or optical maturation); a process by which a material's optical properties are changed as a result of chemical and physical alterations at the surface of grains on airless bodies. Reddened slopes, attenuated absorption bands, and an overall reduction in albedo in the visible and near-IR wavelength ranges are primarily the result of native iron nanoparticle (npFe⁰) production within glassy rims that form from sputtering and vaporization [1-3]. The sizes and abundance of these particles provide information about the relative surface exposure age of a particular grain [3-5]. In addition, many studies have indicated that composition greatly affects the rate at which optical maturation occurs [6-7 and others]. Despite our understanding of how npFe⁰ affects optical signatures, the relative roles of micrometeoroid bombardment and solar wind interactions remains undetermined.

To simulate the early effects of weathering by the solar wind and to determine thresholds for optical change with respect to a given mineral phase, we irradiated a fine-grained lunar basalt with 1 keV H⁺ to a fluence of 6.4×10^{16} H⁺ cm⁻². Surface alterations within four phases have been evaluated using transmission electron microscopy (TEM). We found that for a given fluence of H⁺, the extent of damage acquired by each grain was dependent on its composition. No npFe⁰ was produced in any of the phases evaluated in this study. These results are consistent with many previous studies conducted using ions of similar energy, but they also provide valuable information about the onset of space weathering and the role of the solar wind during the early stages of optical maturation.

Methods: A mounted thin section of Northwest Africa 12008, a low-Ti lunar basalt, was selected for this study. The thin section is primarily composed of small olivine phenocrysts, zoned clinopyroxenes, shocked plagioclase feldspar, and accessory ilmenite. To simulate the effects of the solar wind the sample was irradiated at the Laboratory for Astrophysics and Surface Physics at the University of Virginia under a vacuum of $(4.7 \pm 0.2) \times 10^{-9}$ torr with 1 keV protons with an average flux of $\sim 3.55 \times 10^{12}$ H⁺ cm⁻² s⁻¹ for a fluence of 6.4×10^{16} H⁺ cm⁻². The beam was rastered over an area of 5 ± 1 mm and an electron flood source was used to eliminate sample charging during irradiation.

An FEI Quanta 3D FEG dual beam focused ion beam (FIB) at the NASA Johnson Space Center was used to prepare sections of the irradiated region for TEM imaging. Sections were imaged with JEOL JEM-2500SE and Philips CM200 TEMs.

Results: Mass spectra acquired with a residual gas analyzer during irradiation showed no sputtered ions or neutrals; the lack of detection is likely attributable to sub-optimal detector positioning. Of the four phases evaluated, the augite, plagioclase, and uncharacterized pyroxene exhibited one or more forms of ion-induced damage (Figure 1). The augite developed a ~ 5 nm completely amorphous rim underlain by a partially amorphous region ~ 15 nm in thickness. The already amorphous plagioclase (likely maskelynite) appears to have developed an ~ 8 nm thick rim, but it is unclear at this time how the affected surface differs physically or chemically from the host grain. The uncharacterized pyroxene has also developed a rim, but strain contrast parallel to the sample surface and at a depth of ~ 15 nm, makes this rim difficult to visually interpret. The ilmenite remained unchanged and no gas-induced vesicles were detected at the surface of any mineral phase, consistent with results reported by [6, 8].

Discussion: The three silicate minerals evaluated all developed varying degrees of ion-induced surface damage. The individual rim characteristics, given a single H⁺ fluence, indicate each material has a different threshold value of solar wind ion fluence needed to produce completely amorphous rims. Additional low-fluence studies will help determine the minimum threshold for optically detectable change in grains exposed to the solar wind.

The absence of iron nanoparticles within the rims suggests that low doses of low-energy H⁺ are not capable of producing this alteration, which is ubiquitous in Apollo samples. However, it may be the case that reduction of Fe²⁺ to Fe⁰ by solar wind hydrogen is an essential process in the formation of npFe⁰ produced from micrometeoroid bombardment. These results support the hypotheses of [9-11], who suggest that high albedo regolith associated with lunar swirls is the result of solar wind standoff generated by localized magnetic fields. Because the magnetic fields are not strong enough to redirect micrometeoroids, and because these experimental results indicate that solar wind hydrogen does not produce npFe⁰, it therefore implies that the reduction of iron

prior to micrometeoroid bombardment is essential for the production of npFe^0 in and from vapor deposits.

Summary: A more complete understanding of the role solar wind ions have in the space weathering process makes it possible to more accurately interpret reflectance features on airless bodies. Low fluence experiments are important for interpreting the maturity of returned samples and for determining how and when alterations become optically detectable in remotely acquired spectral reflectance data.

Additional imaging of these samples using an aberration-corrected transmission electron microscope (AC-STEM) will be required to most accurately describe the damage occurring in the plagioclase and in the uncharacterized pyroxene. The ilmenite will also be re-evaluated using AC-STEM to determine if a small, complex, crystalline rim exists as described by [12]. Future work includes re-imaging with AC-TEM/STEM, X-ray photoelectron spectroscopy to denote elemental profiles, and Fourier Transform Infrared spectroscopy measurements to determine the induced optical changes produced at this early stage of alteration.

Acknowledgments: We would like to thank Tony Irving for providing the meteorite sample used in this study. FIB sections were prepared and analyzed using instruments in the Electron Beam Analysis Labs at the NASA Johnson Space Center. We acknowledge the use of facilities within the Eyring Materials Center at Arizona State University.

References: [1] Hapke (2001) *JGR: Planets.*, 106 (E5). [2] Taylor et al. (2001) *JGR: Planets*, 106. [3] Noble et al. (2007) *Icarus*, 192(2). [4] Morris (1978) *Proc. LPS IX*, 2287-2297. [5] Pieters et al. (2000) *Meteoritics & Planet. Sci.*, 35(5). [6] Thompson et al. (2014) *Earth, Planets and Space*, 66(1). [7] Burgess & Stroud (2018) *Geochim. Cosmochim. Acta*, 224. [8] Takigawa et al. (2019) *METSOC*, #2157. [9] Hood & Schubert (1980) *Science*, 208(4439). [10] Kramer et al. (2011) *JGR: Planets*, 116(E4) [11] Glotch et al. (2015) *Nature Comm.*, 6, #6189 [12] Christoffersen et al. (2010) *LPS XLI*, #1532.

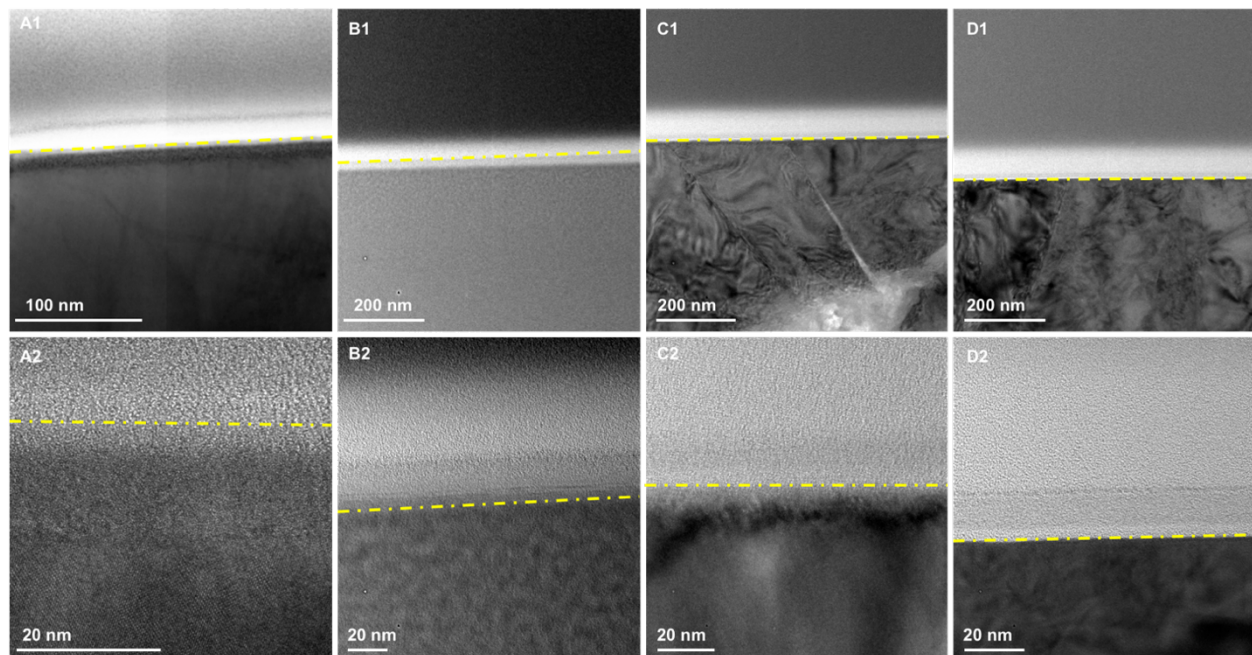


Figure 1. TEM/STEM bright field images of four mineral phases irradiated with 1 keV H^+ : augite (A1 & A2), plagioclase (B1 & B2), uncharacterized pyroxene (C1 & C2), and ilmenite (D1 & D2). Dashed yellow lines indicate the original sample surface.